Supporting Information

Soares-Filho et al. 10.1073/pnas.0913048107

SI Text

Protected Areas of the Brazilian Amazon. There are 12 types of conservation reserves in the Brazilian Amazon biome (1) according to the National Protected Areas System [*Sistema Nacional de Unidades de Conservação* (*SNUC*), law 9985; June 2000]. These types can be grouped into two major categories that can be divided further according to state or national jurisdictions (Table S1): Strictly protected reserves, whose primarily goal is the preservation of biological diversity, comprise ecological stations (*estação ecológica*, ESEC), ecological reserves (*reserva ecológica*, RE), biological reserves (*reserva biológica*, REBIO), state parks (*parque estadual*, PE), and national parks (*parque nacional*, PARNA). Sustainable use reserves, which seek to balance conservation with sustainable use of the natural resources, include sustainable use reserves (*reserva de uso sustentável*, RDS or RESEC), extractive reserves (*reserva extrativista*, RESEX), and areas of significant ecological interest (*área de relevante interesse ecológico*, ARIE). Production forests include state forests (*floresta estadual*, FLOTA or FE), sustained yield forests (*floresta de rendimento sustentado*, FLORSU), extraction forests (*floresta extrativista*, FLOREX), and national forests (*floresta nacional*, FLONA). Environmental Protection Areas (*Áreas de Proteção Ambiental*, APAs) were not included in this study, because they are not in the public domain and thus have less stringent environmental restrictions. Additional benefits of conservation, such as ecosystem services (2), are associated with both categories of protected areas. Of the 320,000 km^2 in protected areas currently supported by the Amazon Protected Areas Program (ARPA) program (a total of 61 areas), 220,000 km^2 are designated as strictly protected, and 100,000 km^2 are designated as sustainable use (Table S1).

The fifth World Parks Congress, promoted by the International Union for Conservation of Nature in Durban, and the Convention on Biological Diversity's (CBD) Program of Work on Protected Areas approved by the Seventh Meeting of the Conference of the Contracting Parties to the Convention on Wetlands refer to protected areas (PAs) *sensu lato* as all those areas that contribute to protect biological diversity even if they have other objectives (3). Under this definition, PAs in the Brazilian Amazon also include indigenous lands and military areas. Indigenous lands in Brazil were established to provide environmental, social, and cultural sanctuaries to indigenous groups. Because of their central role in conserving a large portion of the Amazon biome (23.6% by area), and in accordance with the CBD Program of Work on Protected Areas decision CBD VII/28 (3), indigenous lands can be considered PAs (4). Similarly, military areas also play a relevant role in protecting vast tracts of forests in Brazil, particularly the Serra do Cachimbo military reservation, which covers 22,500 km^2 on the border of the Pará and Mato Grosso states (Fig. S3).

Comparison of Previous Studies of PA Effect on Deforestation. We used the following criteria to compare nine PA studies (5–13): (*i*) number of PAs and level of aggregation (i.e., whether the study provides effectiveness measures for individual PAs, for PA categories, or only for all PAs together); (*ii*) sampling method (e.g., wall-to-wall data versus sampling cells or plots); (*iii*) use of spatial variables to predict deforestation or to adjust PA effectiveness measures, (*iv*) methods used, focusing on whether the method tested and corrected for differences in sampling areas inside and outside PAs; (*v*) statistical assumptions of the methods used and whether these assumptions were tested; and (*vi*) main conclusions (Table S2).

Measuring PA Effectiveness in Reducing Deforestation. Soares-Filho et al. (14) adapted the Bayesian method of conditional probability, known as "weights of evidence" (15), to calculate deforestation probability maps. Since then, this method has been used widely in landscape dynamics simulation models to predict spatially deforestation (16–19) and other land use changes (20, 21).

The posterior probability of deforestation (D) occurring given a presence of a binary spatial pattern (B) (e.g., a protected area) can be denoted as follows:

$$P\{D|B\} = P\{D\} * \frac{P\{B|D\}}{P\{B\}} \quad [1]$$

This equation can be expressed in terms of odds, defined as a ratio of the probability that an event will occur to the probability that it will not occur. For example, the probability of 0.5 of a person winning a contest is equivalent to odds of 0.5/(1–0.5) = 1. Thus, transforming Eq. **1** in odds yields

$$O\{D|B\} = O\{D\} * \frac{P\{B|D\}}{P\{B|\bar{D}\}} \quad [2]$$

where $O\{D|B\}$ is the conditional (posterior) odds of D (deforestation) given a spatial pattern B, and $O\{D\}$is the prior odds of D. The term $P\{B|D\}/P\{B|\bar{D}\}$ is known as the "sufficient ratio" (15). The natural log of this term is the positive weight of evidence, W^+.

The sufficient ratio (here called simply "odds ratio") can be used to assess the relationship between a spatial pattern (e.g., the presence or absence of a PA) and the probability of occurrence of a spatial event D, such as deforestation, simply by computing deforestation inside the spatial pattern and outside it, as in the case of a protected area (B_{PA}), so that

$$O\{B_{PA}|D\} = \frac{D \cap B_{PA} * (\bar{D} \cap B_{PA} + \bar{D} \cap \bar{B}_{PA})}{\bar{D} \cap B_{PA} * (D \cap B_{PA} + D \cap \bar{B}_{PA})} \quad [3]$$

where $D \cap B_{PA}$ is the areal extent of deforestation, and $\bar{D} \cap B_{PA}$ is the areal extent of remaining forest within a PA, $D \cap \bar{B}_{PA}$ is the areal extent of deforestation, and $\bar{D} \cap \bar{B}_{PA}$ is the areal extent of remaining forest outside a PA. Because this expression is a ratio, the unit of measurement (e.g., ha, km^2, cell unit) does not matter. In a similar manner, odds ratios can be calculated for any type of spatial pattern (e.g., soils, distance buffer to roads, elevation ranges) and transformed into W^+, so that the conditional probability of deforestation given the co-occurrence of a set of spatial patterns is denoted as follows:

$$P\{D|B_1 \cap B_2 \cap B_3 \cap ..B_i\} = \frac{e^{(W_d^+ + \Sigma W_i^+)}}{1 + e^{(W_d^+ + \Sigma W_i^+)}} \quad [4]$$

where $P\{D|B_1 \cap B_2 \cap B_3 \cap ..B_i\}$ is the conditional probability of deforestation given a set of spatial patterns ($B_1 . . .B_i$), W_i^+ is the weights of evidence of deforestation occurring for spatial pattern B_i and W_d^+ is the natural log of prior odds of D:

$$O\{D\} = \frac{(D \cap B + D \cap \bar{B})}{(\bar{D} \cap B + \bar{D} \cap \bar{B})} \quad [5]$$

For models in which the deforestation rate is treated as an exogenous variable, there is no need to include $O\{D\}$ in Eq. **4**, because this parameter is the net deforestation rate for a specific area of study, given that $\bar{D}$ represents the remaining forest. The same rationale applies for the calculation of $O\{D|B\}$ for PAs if

we want assess the effect of a PA on deforestation independent of annual variation in the overall deforestation rate (Fig. S2*A*). In this case, $O\{D|B_{PA}\}$ is equal to $O\{B_{PA}|D\}$. Hence, an odds ratio <1 indicates an inhibitory effect for a PA (its conditional probability of deforestation is <0.5), and the effect becomes stronger in magnitude as the odds ratio approaches zero.

The advantage of using this method to assess the role of PA in locally reducing deforestation is that this spatial metric is independent of the variation of the overall deforestation rate and is sensitive to the variations in size of the areas being compared inside and outside the PA as well as to the PA location with respect to the Arc of Deforestation (eastern, southern, and southwestern Amazon). Moreover, this metric is not constrained by the assumptions of parametric methods (such as linear or logistic regressions), which spatial data often violate (22). The only assumption for this Bayesian method consists of conditional independence between the spatial patterns B_i, which can be tested using pairwise tests, such as the Crammer's coefficient (15). The odds ratio of deforestation occurring can be calculated for a single PA, for a group of PAs of the same category, or for all PAs, and these results then can be tested for statistical significance, so that a W_i^+ value is statistically significant within a confidence interval of 95% if $|W_i^+| > 1.96 * \mathrm{SE}$ (23), where the *SE* is

$$SE = \sqrt[2]{\frac{1}{N\{D \cap B\}} + \frac{1}{N\{\bar{D} \cap B\}}} \qquad [6]$$

where $N\{D \cap B\}$ is the number of occurrences of D in spatial pattern B, and $N\{\bar{D} \cap B\}$ is the number of occurrences of $\bar{D}$ in spatial pattern B. This approximation is asymptotic and thus will not give a meaningful result if any of the area counts are very small.

A disadvantage is that this method requires a sufficiently large training data set, implying wall-to-wall deforestation data with fine spatial resolution. As such, we can show that resampling the Programa de Cálculo do Desflorestamento da Amazônia (PRODES) original spatial resolution of 0.36 ha may affect the results, especially for small areas, because the resampling process tends to omit small deforestation patches. For example, the mean odds ratio for RESEX do Curralinho is 1.07 at 25 ha and 0.33 at 0.36 ha spatial resolution. In addition, continuous gray-tone variables must be categorized in spatial patterns B_i to calculate weights of evidence. Nevertheless, this calculation can be achieved easily using an optimization method available in Soares-Filho et al. (24).

PA Pairwise Comparison Method. Comparisons of interior versus exterior of deforestation can be biased: Landscape characteristics in sampled areas are not the same because the locations of PAs usually are more remote (25) and thus are less likely to be deforested than exterior areas (11–13). To overcome this limitation, we confined our analyses of inhibitory effect to the 10-km buffer zones immediately inside and outside PAs, where landscape characteristics should be approximately the same. To test this assumption, we integrated the effects of a series of spatial determinants [so-termed because they represent proximate causes of deforestation (e.g, the opening or paving of a road), or simply are preferable (e.g., have more fertile soil or flat terrain), or are restricted sites (land use zoning, such as PAs)] into a probability map of deforestation. This approach is similar to the logistic regression method used to calculate propensity scores (12), although it is not parametric, and thus takes into account the differential effects of spatial determinants on the spatial prediction of deforestation.

Among the various factors that influence the location of deforestation in the Amazon (14, 16), we chose the following variables: (*i*) distance to rivers, (*ii*) distance to major roads, (*iii*) maximum net present value (MNPV) from soy and cattle rents (26), (*iv*) suitability of soil and terrain for mechanized crops (27), (*v*) elevation, (*vi*) slope; and (*vii*) attraction by urban centers, which is an output from a gravitational model of urban centers, where urban population is the mass of urban center *i* as follows: $\sum \mathrm{Mass}_i/\mathrm{distance}_i$ (16). Distance to vicinal roads and population density were not included, because the creation of a PA prevents roads being built and people moving in.

First, we tested these variables for spatial dependence by using the Crammer's coefficient (15), and because they showed little spatial dependence (only suitability of soil and terrain for mechanized farming with MNPV showed a certain level of spatial association, still <50%), we derived weights of evidence for them. The differential effects of these variables on the location of deforestation, as represented by their weights of evidence coefficients, are integrated by using Eq. **4** to produce a probability map. We performed the weights of evidence analysis using deforestation data up to 1997 and validated the resulting probability map by simulating deforestation with the Brazilian Amazon rates from 1997–2008. The method we used to validate the simulation is known as the "reciprocal fuzzy comparison" (24, 28). It evaluates the spatial match between the observed changes and simulated ones within map windows of increasing size. As a result, the model showed a spatial fitness of 70% at a window size of 7.5 km, meaning that it can predict accurately the location of 70% of the Brazilian Amazon deforestation (1997–2008) at a 7.5-km search radius.

Next, for each PA we compared the distributions of deforestation probability in the 10-km buffer zones immediately within and outside the PA border. In general the pairs of 10-km adjacent buffers presented close mean probabilities of deforestation, yielding a regression with R^2 of 0.945 and β_0 slightly exceeding 1 ($y = 1.027x$). Nevertheless, 453 of 571 pairs turned out to have different distributions according to both Kolmogorov-Smirnov and Kruskal-Wallis tests (95% confidence interval). These results suggest the need to compensate for the differences in conditional probabilities in the areas of comparison. One approach would be to try to find matching samples. However, because the PAs in the Brazilian Amazon form a complex and interlocking mosaic, this strategy would prove difficult. Statistical tests show that most pairs of 10-km adjacent buffers have different distributions of probability, suggesting that we should look for potential matching samples at a distance from PA boundaries, both inside and outside the PA. The conditional probability of deforestation tends to increase from PAs toward major roads and towns, making it virtually impossible to find a sufficiently large number of samples (that could yield statistically significant results) with equivalent deforestation probabilities in a particular PA and its area of influence. A feasible alternative approach consists of adjusting the odds ratio to compensate for differences in deforestation probability in areas used for pairwise comparison. The weights of evidence method integrates the effects of all spatial determinants by summing their weights of evidence (including the ones of PAs) to produce the probability map. In next section we show that this calculation also can be used to generate an adjusted odds ratio, in which the conditional probability of deforestation becomes embedded.

Odds Ratio of Deforestation Adjusted to Compensate for Differences in Deforestation Probability in Areas Used for Pairwise Comparison. To account for differences in the probability of deforestation in the areas used for pairwise comparison, we can convert their conditional deforestation probabilities (Eq. **4**) into sums of weights of evidence, which represent the integrated effect of other factors (but not PA status) on deforestation and subtract the sum of weights of the internal buffer from that of the external buffer, as follows: $\Delta W^+ = \sum W^+_{i(out)} - \sum W^+_{i(in)}$. Then the term ΔW^+ is added to the summation of Eq. **4** to adjust the conditional probability of deforestation of the PA internal

buffer. This calculation also can be performed using the ratio between the conditional odds of deforestation in the interior and exterior buffer zones, so that an adjusted PA odds ratio is

$$O\{B_{PA}|D\}_{adjusted} = O\{B_{PA}|D\} * O\{D|B_1 \cap .. B_i\}_{out} / O\{D|B_1 \cap .. B_i\}_{in} \quad [7]$$

where $O\{D|B_1 \cap .. B_i\}_{out}$ and $O\{D|B_1 \cap .. B_i\}_{in}$ represent the mean conditional odds ratios of deforestation, when controlling for a group of spatial determinants in the internal and external buffers. Replacing $O\{B_{PA}|D\}$ in Eq. **7** with Eq. **3** yields the following:

$$O\{PA|D\}_{adjusted} = \frac{O\{D|B_1 \cap .. B_i\}_{out} * D \cap B_{PA} * (\bar{D} \cap B_{PA} + \bar{D} \cap \bar{B}_{PA})}{O\{D|B_1 \cap .. B_i\}_{in} * \bar{D} \cap B_{PA} * (D \cap B_{PA} + D \cap \bar{B}_{PA})} \quad [8]$$

Algebraic manipulation of Eq. **8** leads to

$$O\{PA|D\}_{adjusted} = \frac{\begin{pmatrix} D \cap B_{PA} * \bar{D} \cap B_{PA} * O\{D|B_1 \cap .. B_i\}_{out} * D \cap \bar{B}_{PA} + \\ D \cap B_{PA} * D \cap \bar{B}_{PA} * O\{D|B_1 \cap .. B_i\}_{out} * \bar{D} \cap \bar{B}_{PA} \end{pmatrix}}{\begin{pmatrix} D \cap \bar{B}_{PA} * \bar{D} \cap B_{PA} * O\{D|B_1 \cap .. B_i\}_{in} * D \cap B_{PA} + \\ (D \cap \bar{B}_{PA})^2 * O\{D|B_1 \cap .. B_i\}_{in} * \bar{D} \cap B_{PA} \end{pmatrix}} \quad [9]$$

Instead of using single mean values for $O\{D|B_1 \cap .. B_i\}_{out}$ and $O\{D|B_1 \cap .. B_i\}_{in}$ for adjusting $O\{PA|D\}$, considering that the average is a statistical measure that does not necessarily differentiate unlike populations, the previous equation can be transformed into a summation, which enables us to compute the conditional odds ratios of all spatial determinants of deforestation at a cell *x,y* continuously across the space as follows:

$$O\{PA|D\}_{adjusted} = \frac{\begin{pmatrix} D \cap B_{PA} * \bar{D} \cap B_{PA} * \sum(O\{D|B_1 \cap .. B_i\}_{out} * D \cap \bar{B}_{PA}) + \\ D \cap B_{PA} * D \cap \bar{B}_{PA} * \sum(O\{D|B_1 \cap .. B_i\}_{out} * \bar{D} \cap \bar{B}_{PA}) \end{pmatrix}}{\begin{pmatrix} D \cap \bar{B}_{PA} * \bar{D} \cap B_{PA} * \sum(O\{D|B_1 \cap .. B_i\}_{in} * D \cap B_{PA}) + \\ (D \cap \bar{B}_{PA})^2 * \sum(O\{D|B_1 \cap .. B_i\}_{in} * \bar{D} \cap B_{PA}) \end{pmatrix}} \quad [10]$$

As a result, Eq. **10** incorporates differences in the conditional probability of deforestation in both forested and deforested cells of the areas of pairwise comparison independent of the cell location. In addition, it continues to incorporate all features of the Bayesian weights of evidence method and therefore can be applied straightforwardly to a basin-wide assessment of PAs (Fig. S3). We demonstrate the simplicity of this method by making available for download a sequence of models designed with Dinamica EGO (for "Environment for Geoprocessing Objects"). Dinamica EGO freeware contains a series of spatial algorithms for the analysis and simulation of space–time phenomena (24). Its graphical interface allows the design of a model simply by dragging and connecting operators that perform some calculation upon various types of data, such as constants, matrices, tables, and raster maps. Software, models, and a demonstration dataset (25 ha spatial resolution) are available for download upon request to the corresponding author.

Analyzing Spatial Dependence Between the Creation of PAs and Deforestation. We did a binary test for 50-km cells where PAs expanded (Fig. S5*A*) and for cells where deforestation increased (Fig. S5*B*). According to the K12 test (29), increase in extent of PA and increase in deforestation outside of PAs were not spatially dependent, as demonstrated by the fact that the K12 function fell within the confidence envelope. In addition, we evaluated the spatial dependence between maps of percent in PA increase versus the maps of percent in deforestation reduction and increase applying the Cramer's coefficient and Cramer's contingency coefficient pairwise tests (15) (Fig. S5 *A–D*). This assessment used 50-km cell maps as well as Amazon municipality maps. The use of both approaches ensured that a wide range of PA coverage is represented within the spatial units of analysis (Fig. S5*D*). Neither of the Cramer indices indicated spatial dependence between the maps (all values were <50%), and the indices showed even less spatial dependence when we compared the map of increase in deforestation with the map of PA expansion. As a result, no spatial dependence was found between areas where PAs expanded and the few areas in the Amazon where deforestation increased contrary to the overall declining trend (Fig. S5 *A–D*).

Modeling PA Contribution to the Recent Decline in the Amazon Deforestation Rates. ***Model development.*** Our econometric model analyzes the influence of a series of socioeconomic and demographic variables [selected from 1996 and 2000 Instituto Brasileiro de Geografia e Estatísticas (IBGE) censuses and from other economic and social surveys carried out within this period] on the deforestation trend. This dataset includes the following variables: (*i*) proximity to paved road and (*ii*) urban attraction (source of *i* and *ii*: refs. 16 and 26); (*iii*) density of cattle herd [source: IBGE Pesquisa Pecuária Municipal (PPM) municipal cattle herd surveys, 1997 and 2001 (30)], (*iv*) percentage of crop areas [source: IBGE Pesquisa Agrícola Municipal (PAM) municipal agricultural survey, 1997 and 2001 (30)], (*v*) crop rent, (*vi*) percentage of jobs in the agricultural sector, and (*vii*) land concentration (large landholders/small land holders) [source of *v–vii*: IBGE 1995–1996 agricultural census (30)]; (*viii*) total population density, (*ix*) rural population density, (*x*) rural population density, (*xi*) urbanization level, (*xii*) net migration rate (1995/2000), and (*xiii*) migratory volume (1995/2000) [source of *viii–xiii*: IBGE 1996 population tally and IBGE 2000 demographic census (30)]; (*xiv*) domestic gross product (30) and percentage of protected area. Data from command and control programs (31) could not be included, because this information is classified. This data set was assembled for each Brazilian Amazon municipality together with PRODES wall-to-wall deforestation data from 1997–2001 (32), which were aggregated at the municipal level to comprise the dependent variable.

To account for the large variation in the size of the Amazon municipalities, we weighted some variables that depend greatly on the size of the sampling unit by municipality area to produce, for example, densities of cattle herd, percent of crop areas, and density of rural population. Deforestation, the dependent variable, also was transformed into a percentage by area. We began by analyzing two models: one relating stocks of the independent variables with the percent of deforested area, and the other relating the net deforestation rate (1997–2001 gross deforestation rates in hectares divided by the municipality's original forest area) with changes in the socioeconomic context. In both cases, we excluded municipalities outside the Amazon forest biome as well as those with lack of data resulting from gaps in PRODES mapping or cloud coverage problems. By this approach we aimed to reduce uncertainties in the early PRODES phase, whose methodology was based solely on visual interpretation. The first model is subject to temporal dependence: Similar to the chicken-and-egg dilemma, we cannot assert which variable (e.g., deforested area or density of cattle herd) is cause, and which is effect. Hence, we used only the second model, which is devoid of temporal dependence, because it relates rates of deforestation with rates of change of socioeconomic variables (33).

To adapt the model better to our knowledge, we adopted an ad hoc criterion of inclusion and exclusion of variable to the stepwise regression results. The criterion consists of interrupting the variable swapping process when the R^2 of the best-fit stepwise regression is reduced by 5%. After variable selection the model

passed a heteroskedastic control and was tested for spatial autocorrelation using Moran's I, Lagrange Multiplier, and Robust LM tests (34). Because the model failed the autocorrelation tests, we removed this effect by developing a spatial lag regression as follows:

$$y = \rho W y + X\beta + \varepsilon \quad [11]$$

Where ρ is the autoregressive coefficient, W is a first-order neighborhood matrix, y is the dependent variable, X is the matrix of observations for the independent variables, β is the vector of regression coefficients, and ε is a random error term (34).

As a result, the final regression model achieved an R^2 of 0.64 (Table S3). Proximity to paved roads, change in cattle herd density, change in percent of crop areas, net migration rates, and percent of protected areas were the most important variables in explaining the deforestation rates within the 1997–2001 period, with only the last exhibiting a negative relationship to deforestation rates.

Model validation. In model validation it is necessary to use data that were not used in the calibration process. Therefore, we validated the model projecting annual deforestation rates from 2002–2006, using a series of socioeconomic data (change in cattle herd, change in percent of crop areas) obtained from annual IBGE surveys (Fig. S1 *A* and *B*) and the percent increase of area in PAs within the municipality as a result of the recent expansion of the Amazon PA network (Fig. 1 and Fig. S1*C*). The other two variables (net migration rate and proximity to paved road) were kept constant, because they did not experience significant alteration during the 2002–2006 period.

We had to adapt the model for the validation process. First, the term ρ*Wy* (Eq. **11**) had to be calculated in an iterative way using moving averages of the y responses from the neighboring municipalities. Second, because variables cover 4 years (1997–2001) of deforestation, we fixed the rates of changes of the independent variables for a period of 4 years to project their effects and then divided the resulting gross deforestation rate by 4 to scale to annual output.

Following these adaptations, it was anticipated that the deforestation rates from the model would respond quickly to the variations in rates of cattle herd growth and crop expansion and to the percentage of municipality area covered by PA (Fig. S1*D*). Both the size of the cattle herd and the area in cropland expanded rapidly in the Amazon from the beginning of this decade until 2005, when the soy market crashed, severely impacting the Brazilian agricultural sector (Fig. S1 *A* and *B*). In turn, of a 5.1 million km^2 area that corresponds to 792 Amazon municipalities, the PA network expanded from 19% in 2001 to 23% in 2002, 25% in 2003, 29% in 2004, 30% in 2005, and 35% in 2006 (Fig. S1*C*).

Modeling PA Contribution to the Recent Decline in Deforestation Rates. Fig. S4 *A* and *B* shows differences from 2001–2004 and from 2004–2006, respectively, in projected deforestation for Amazon municipalities, given rates of change of the cattle herd, crop area, and percent of the municipality in PAs during each period. Fig. S4*A* shows that most of the municipalities experienced an increase in deforestation between 2002 and 2004, especially along the Arc of Deforestation. This trend then reversed during the period 2004–2006, with most municipalities exhibiting a decline in deforestation (Fig. S4*B*). To separate the effect of PA expansion from the effect of the deceleration of the agricultural sector on deforestation during the same period, we ran two models with data from 2006, first excluding the PA expansion that occurred during this period (using PA data from 2004 instead of 2006) and then replacing the values for cattle herd growth and rate of increase in crop areas for 2006 with those for 2004. Finally, for each of the alternate models for 2006, we compared the difference between predicted deforestation rates and observed deforestation rates during the same period (Fig. S4 *C* and *D*). As a result, municipalities where PA expansion had greater influence on the reduction in the deforestation rate show negative values in Fig. S4*C* , and municipalities where agricultural influence was stronger show negative values in Fig. S4*D*.

Simulating the Future Contribution of PAs to Reducing Deforestation in the Brazilian Amazon. We coupled the econometric projection model to SimAmazonia (16). In this model, called "SimAmazonia-2," deforestation rates are projected based on scenarios of agricultural growth, protected area network, migration, and infrastructure improvement. The two socioeconomic scenarios—high and moderate growth—involve, respectively, the following assumptions: (*i*) mean annual rate of cattle herd expansion: 5% year^{-1} and 2% year^{-1}; (*ii*) mean annual rate of crop expansion: 5% year^{-1} and 2% year^{-1}; (*iii*) internal migration rates: 1996–2000 rates and no migration; (*iv*) extent of road paving expansion: 14,000 km and 11,500 km [thus excluding the paving of BR-163 Trairão from the Mato Grosso border, BR-230 from Itaituba to Humaitá, BR-319 Manaus-Porto Velho, and BR-230 Perimetral Norte (16)]. Because this model incorporates a neighborhood matrix, it can be used to infer potential for future deforestation in a specific Amazon municipality not only from changes in its socioeconomic and demographic context but also in the context of its neighboring municipalities. To simulate future deforestation trajectories, the model was adapted to constrain rates of cattle herd and crop growth by available agricultural land in each municipality. Next, the gross deforestation rates predicted by the model were aggregated for subregions (35) to be used as an input in a spatially explicit model (the SimAmazonia-2 transition module consists of a Cellular Automata model (36) that runs at a spatial resolution of 100 ha per cell) that integrates the influence of a set of spatial determinants such as elevation, slope, rivers, vegetation, soils, climate, infrastructure, towns, and land-use zoning (e.g., presence or absence of a category of PA) to predict the location of deforestation (14, 16). The area-weighted mean effect per category of PA (Table 1), measured in the odds ratio of deforestation and then transformed into weights of evidence, is used for this calculation. In this case, the model employs the odds ratios before adjustment, because the effects of other spatial determinants also are taken into account in the computation of Eq. **4**. SimAmazonia-2 also is implemented with Dinamica EGO freeware (24).

The scenario of exclusion of all current PAs aims to determine which PAs would be most susceptible to deforestation if they did not, in fact, protected; hence, its outcome shows where PAs are extremely effective in slowing the advance of deforestation. Because this effect is time-dependent (the deforestation frontier will reach different PAs at different times), we established an index to calculate the threat posed by future deforestation, as follows:

$$\textit{Level of threat} = 100 * \frac{\textit{model final time} + 1\textit{-year that a cell is deforested}}{\textit{model final time} + 1\textit{-model initial time}} \quad [12]$$

Opportunity Costs of Protected Areas. To estimate the opportunity costs for preventing forest conversion to agricultural land (Dataset S1), we applied a set of spatially explicit dynamic models of potential rents from soy, cattle, and timber production (26, 37).

We incorporated uncertainty bounds in the rent estimates, running the models within a range of input prices: the cattle model with the lowest and highest annual mean cattle and beef prices from 2002–2009 for the Brazilian Amazon states (US$1.70 ± 0.14 to US$2.58 ± 0.27 kg^{-1} www.cepea.esalq.usp.br), the soy model with historical recent low (2002–2006) and high

(2007–2009) average soy prices (US$229–335 ton^{-1} freight on board; www.cisoja.com.br), and the logging model [because no price series is available for the major Amazon milling centers, we first used fixed 2004 sawnwood prices (38) and then projected these prices into the future using their 1998–2004 annual growth rate of 1.5% (39)].

The timber rent model consists of a 30-year, partial equilibrium, spatial simulation model of the Amazon timber industry, which calculates a residual stumpage value on forest lands, an annual harvest volume and value, and potential tax revenues and thereby forecasts industrial capacity (38). A residual analysis is used to calculate standing tree value or forest rent for each land unit. Commercial volume is estimated for each land unit using available geographical data and an initial demand corresponding to current logging capacity of processing centers. Processing centers are assumed to be located at municipal seats. A sawnwood price at the mill gate is specified for each processing center, and the model works recursively for each land unit, deducting transport costs for wood from the land unit to the mill gate. The resulting value is the potential net rent from harvesting a particular forest land unit in a given location at a given point in time. This value is known in economics as a "residual" or "stumpage" price. This stumpage price is multiplied by commercial volume at each land unit to arrive at an estimate of forest rent for the land unit. Furthermore, the model can force the industry into a sustainable mode, assuming that each processing center will harvest only 1/30th of its available volume.

The cattle ranching model integrates a herd development model and a production rent function that includes initial ranch infrastructure, herd acquisition, and periodic cattle maintenance costs and sale revenues (26). The model is designed to simulate the 30-year net present value (NPV) of extensive cattle ranching for a given land parcel in the Brazilian Amazon. To arrive at this figure, we developed a spatially and temporally explicit profit function that reflects the fixed and variable costs associated with extensive cattle ranching in the region. Annual profit is calculated for each year that the model runs and then is discounted to the initial year and summed over the 30-year time horizon of the model to arrive at a NPV figure for a given land parcel. We assume that, in the initial year, the agent acquires (either through purchase or occupation) and deforests the land. Following the process of deforestation and land clearing, we assume that some upfront investment in property infrastructure is required (e.g., construction of fences and roads, a corral, water and feeding troughs). We estimate the value of these costs on a per-hectare basis by making reasonable assumptions about the level and type of type of investments made by a representative rancher with a 3,000-ha property. Rather than assume that the representative rancher has sufficient financial capital on hand to clear land, build roads, and make all required investments, we simulate these investments over the first 12 years of the model using an annual loan repayment schedule specific to the interest rate and grace and repayment periods for different types of agricultural credit. In addition, we incorporate maintenance for each type of infrastructure into annual (variable) costs. Similarly, we distribute the cost of purchase of a sufficient number of cows and bulls to give rise to and maintain a self-sustaining herd for beef production over the first few years of the model. Annual (variable) costs include infrastructure maintenance, taxes on the value of animal sales and on productive land, and wages for a manager and ranch hands. The largest portion of annual costs comprises the costs of vaccinating and maintaining the herd. We simulate spatially variable transportation costs for production inputs using a percent markup over input price to a maximum of 1.5 times the cost of the original input. Cost increases proportionally to distance along paved roads and then increases more than proportionally to distance for cells that are more removed from the road until it reaches the maximum cost. The cost of transporting animals from a given land parcel to a slaughterhouse location is simply the cost of transportation per animal kilometer^{-1} multiplied by the distance to slaughter. Annual revenue from sales of each type of animal and density of heads per land parcel compose the NPV figure hectare^{-1}.

To estimate soybean crop rents, we applied an interdisciplinary model based on climate, soils, and economic variables (40). This model comprises a component of soybean yield that integrates the major climatic, edaphic, and economic determinants for soy crops in the Amazon Basin. Yield is simulated using a crop physiology model that captures the effects of climate and physical attributes on the development of soybean plants (40). Coupled to the yield component is a rent model that deducts the costs of soybean production (e.g., fertilizer applications and credit costs) and transportation to exportation ports from its market price; the result then is multiplied by the expected productivity hectare^{-1} output by the yield component. We adapted this model to simulate soybean profitability over a 30-year period based on variation in transportation costs resulting from road expansion and paving throughout the Amazon region (16). We then constrained the soy rent model to produce positive rents only on land suitable for mechanized agriculture. The suitability map for mechanized agriculture takes into account four factors (27): the availability of flat land, appropriate soils, inundation-free areas, and regions without climatic restrictions. The first factor was obtained deriving the Shuttle Radar Topography Mission topography to produce an altitude deviance map and then visually setting a threshold to identify the flat lands. As a last step, a mode filter was applied to eliminate small areas, because mechanized agriculture requires large tracts of land. Soil criteria excluded soils with strong edaphic restrictions (e.g., ultisols, lithosols, dysthropic podzols, sands, and hydromorphic soils). Flooding plains were mapped by expanding the altitudes on the major river channels to the surrounding regions and then defining a flooding threshold equal to the river altitudes plus 10 m. Finally, regions with average annual precipitation above 2,250 mm or above 0.5 mm day^{-1} during the 4 driest months were masked from the combined map, because they are too rainy to develop large-scale crops.

1. Ministério do Meio Ambiente (2004) *Project on Conservation and Sustainable Utilization of the Brazilian Biodiversity* (Ministério do Meio Ambiente, Brasília, Brazil) (in Portuguese).
2. Costanza R, et al. (1997) The value of world's ecosystem services and natural capital. *Nature* 387:253–260.
3. Convention on Biological Diversity, Ad Hoc Open-Ended Working Group on Protected Areas (2007) *Review of Implementation of the Programme of Work on Protected Areas for the Period 2004–2007* (United Nations Food and Agriculture Organization, Rome), pp 1–16.
4. Maretti CC (2004) *Indigenous Lands and Nature Conservation Units: The Challenge of Superposition*, ed Ricardo F (Instituto Socioambiental, São Paulo, Brazil), pp 85–101 (in Portuguese).
5. Curran LM, et al. (2004) Lowland forest loss in protected areas of Indonesian Borneo. *Science* 303:1000–1003.
6. Pfaff ASP, Sanchez-Azofeifa GA (2004) Deforestation pressure and biological reserve planning: A conceptual approach and an illustrative application for Costa Rica. *Resource and Energy Economics* 26:237–254.
7. DeFries R, Hansen A, Newton AC, Hansen MC (2005) Increasing isolation of protected areas in tropical forests over the past twenty years. *Ecol Appl* 15:19–26.
8. Nepstad DC, et al. (2006) Inhibition of Amazon deforestation and fire by parks and indigenous lands. *Conserv Biol* 20:65–73.
9. Oliveira PJ, et al. (2007) Land-use allocation protects the Peruvian Amazon. *Science* 317:1233–1236.
10. Joppa LN, Loarie SR, Pimm SL (2008) On the protection of "protected areas". *Proc Natl Acad Sci USA* 105:6673–6678.
11. Andam KS, Ferraro PJ, Pfaff A, Sanchez-Azofeifa GA, Robalino JA (2008) Measuring the effectiveness of protected area networks in reducing deforestation. *Proc Natl Acad Sci USA* 105:16089–16094.
12. Gaveau DLA, et al. (2009) Evaluating whether protected areas reduce tropical deforestation in Sumatra. *J Biogeogr* 36:2165–2175.
13. Pfaff A, Robalino J, Sanchez-Azofeifa GA, Andam KS, Ferraro PJ (2009) Park location affects forest protection: Land characteristics cause differences in park impacts across

Costa Rica. *B E J Econom Anal Policy*. Available at http://www.bepress.com/bejeap/vol9/iss2/art5/. Accessed April 6, 2010.
14. Soares-Filho BS, et al. (2004) Simulating the response of land-cover changes to road paving and governance along a major Amazon highway: The Santarém-Cuiabá corridor. *Global Change Biology* 10:745–764.
15. Bonham-Carter G (1994) *Geographic Information Systems for Geoscientists: Modelling with GIS* (Pergamon, New York).
16. Soares-Filho BS, et al. (2006) Modelling conservation in the Amazon basin. *Nature* 440:520–523.
17. Cuevas G, et al. (2008) in *Modelling Environmental Dynamics*, eds Paegelow M, Camacho Olmedo MT (Springer, Heidelberg), pp 223–246.
18. Texeira AM, et al. (2009) Modeling landscape dynamics in the Atlantic Rainforest domain: Implications for conservation. *For Ecol Manage* 257:1219–1230.
19. Stickler C, et al. (2009) The potential ecological costs and co-benefits of REDD: A critical review and case study. *Global Change Biology* 15:2803–2824.
20. Almeida C, et al. (2005) GIS and remote sensing as tools for the simulation of urban land use change. *Int J Remote Sens* 26:759–774.
21. Godoy M, Soares-Filho BS (2008) in *Modelling Environmental Dynamics*, eds Paegelow M, Camacho Olmedo MT (Springer, Heidelberg), pp 319–338.
22. Hagget P, Cliff AD, Frey A (1977) *Locational Analysis in Human Geography* (Wiley & Sons, New York).
23. Goodacre CM, Bonham-Carter GF, Agterberg FP, Wright DF (1993) A statistical analysis of spatial association of seismicity with drainage patterns and magnetic anomalies in western Quebec. *Tectonophysics* 217:205–305.
24. Soares-Filho BS, Rodrigues H, Costa W (2009) *Modeling Environmental Dynamics with Dinamica EGO*. Available at www.csr.ufmg.br/dinamica. Accessed April 6, 2010.
25. Margules CR, Pressey RL (2000) Systematic conservation planning. *Nature* 405: 243–253.
26. Nepstad DC, et al. (2009) Environment. The end of deforestation in the Brazilian Amazon. *Science* 326:1350–1351.
27. Nepstad D, Stickler C, Soares-Filho BS, Brando P, Merry F (2008) Ecological, economic, and climatic tipping points of an Amazon forest dieback. *Philos Trans R Soc Lond B Biol Sci* 363:1737–1746.
28. Almeida CM, Gleriani JM, Castejon EF, Soares-Filho BS (2008) Using neural networks and cellular automata for modeling intra-urban land use dynamics. *International Journal of Geographical Information Science* 22:943–963.
29. Bailey TC, Gatrell AC (1995) *Interactive Spatial Data Analysis* (Longman, New York).
30. Instituto Brasileiro de Geografia e Estatística (2008) IBGE – SIDRA: Sistema IBGE de Recuperação Automática. Available at http://www.sidra.ibge.gov.br/bda/default.asp. Accessed May 14, 2010.
31. Casa Civil (2004) Action plan for the control and prevention of deforestation in the legal Amazon. Available at www.planalto.gov.br/casacivil/desmat.pdf. Accessed April 6, 2010 (in Portuguese).
32. Instituto Nacional de Pesquisas Espaciais (2009) PRODES: Assessment of deforestation in Brazilian Amazonia. Available at http://www.obt.inpe.br/prodes/. Accessed February 1, 2010.
33. Soares-Filho BS, Garcia RA, Rodrigues H, Moro S, Nepstad D (2008) in Amazonia: Nature and Society in Transformation, eds Batistella M, Moran EF, Alves D (Edusp, São Paulo), pp 181–220 (in Portuguese).
34. Anselin L (2002) *Spatial Externalities, Spatial Multipliers and Spatial Econometrics* (Univ of Illinois, Urbana-Champaign, IL).
35. Garcia RA, Soares-Filho BS, Swayer D (2007) Socioeconomic dimensions, migration, and deforestation: An integrated model of territorial organization for the Brazilian Amazon. *Ecological Indicators* 7:719–730.
36. Soares-Filho BS, Pennachin CL, Cerqueira G (2002) DINAMICA – a stochastic cellular automata model designed to simulate the landscape dynamics in an Amazonian colonization frontier. *Ecol Modell* 154:217–235.
37. Nepstad D, et al. (2007) *The Costs and Benefits of Reducing Carbon Emissions from Deforestation and Forest Degradation in the Brazilian Amazon. Report launched in the United Nations Framework Convention on Climate Change (UNFCCC), December 3–15, 2007.* (Conference of the Parties 13th session, Bali, Indonesia).
38. Merry F, Soares-Filho BS, Nepstad D, Amacher G, Rodrigues H (2009) Balancing conservation and economic sustainability: The future of the Amazon timber industry. *Environ Manage* 44:395–407.
39. Lentini M, Pereira D, Celentano D, Pereira R (2005) *Amazon forest facts* (IMAZON, Belém, Brazil). Available at http://www.imazon.org.br/downloads/. (in Portuguese).
40. Vera-Diaz M, Kaufmann R, Nepstad D, Schlesinger P (2008) An interdisciplinary model of soybean yield in the Amazon Basin: The climatic, edaphic, and economic determinants. *Ecol Econ* 3:420–431.

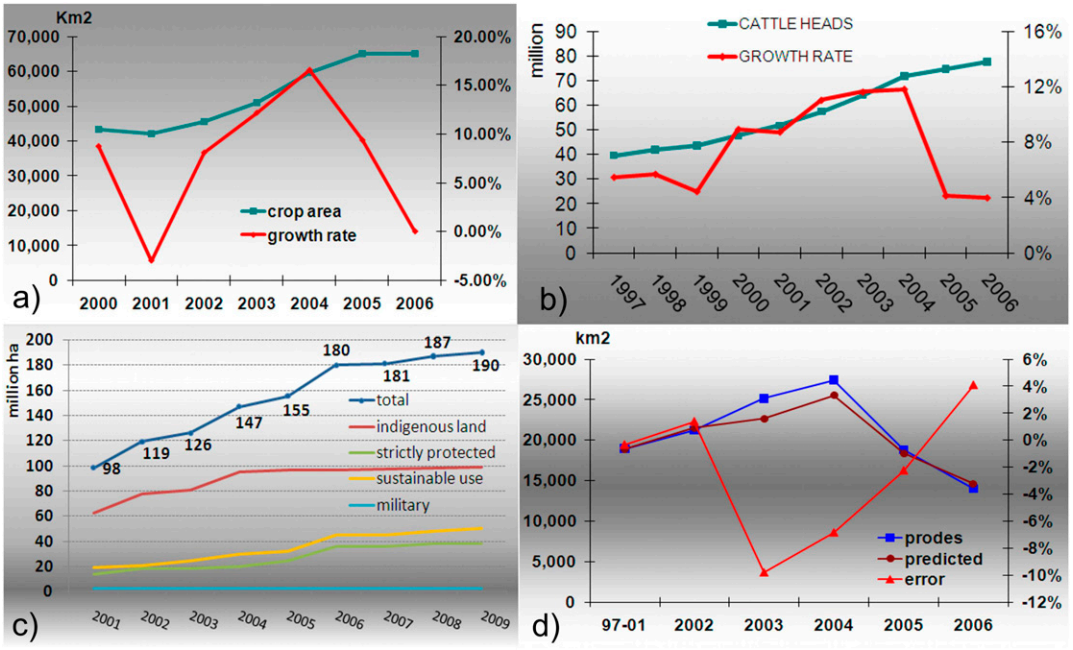

Fig. S1. Variation in the socioeconomic context, PA expansion, and model validation. (*A*) Recent crop area expansion in the Amazon (1). (*B*) Recent cattle herd expansion in the Amazon (2). (*C*) PA expansion in the Brazilian Amazon from 2001–2009. (*D*) Model validation.

1. Instituto Brasileiro de Geografia e Estatística (2008) IBGE – PAM: Pesquisa Agropecuária Municipal. Available at http://www.sidra.ibge.gov.br/bda/pesquisas/pam/. Accessed May 14, 2010.
2. Instituto Brasileiro de Geografia e Estatística (2008) IBGE – PPM: Pesquisa Pecuária Municipal. Available at http://www.sidra.ibge.gov.br/bda/pesquisas/ppm/. Accessed May 14, 2010.

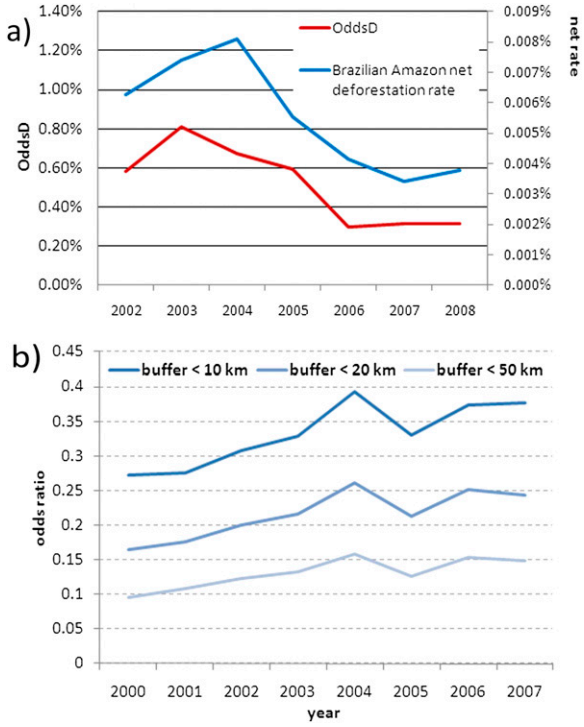

Fig. S2. Odds ratios of deforestation. (*A*) Prior odds ratio of deforestation in a 10-km buffer both inside and outside the PA boundary (OddsD). Note that this metric is influenced by the Brazilian Amazon overall rate of deforestation. (*B*) Odds ratios of deforestation in PAs, when analyzing data in PAs and in adjacent buffer zones of 10, 20, and 50 km, before adjusting the odds ratio to incorporate the effect of other spatial determinants of deforestation. Annual variation in odds ratios reflects different proportions of deforestation over time in areas of comparison inside and outside PAs.

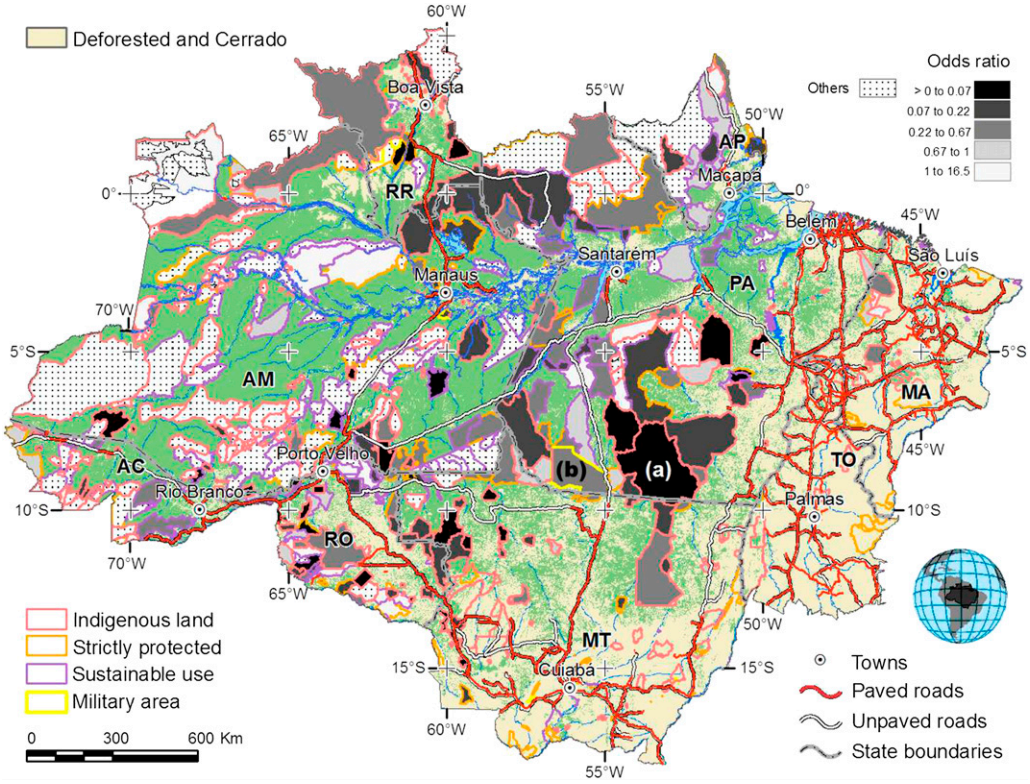

Fig. S3. Mean adjusted odds ratios of deforestation in PAs (1997–2008). Note the inhibitory effect of indigenous lands, such as the Xingu/Jarina/Menkragnotí/Kayapó/Baú complex in the central part of Mato Grosso and Pará (*A*) and the Serra do Cachimbo reservation (*B*). Other items in the legend represent non-significant values and zero odds ratios. AC, Acre; AM, Amazonas; AP, Amapá; MA, Maranhão; MT, Mato Grosso; PA, Pará; RO, Rondônia; RR, Roraima; TO, Tocantins.

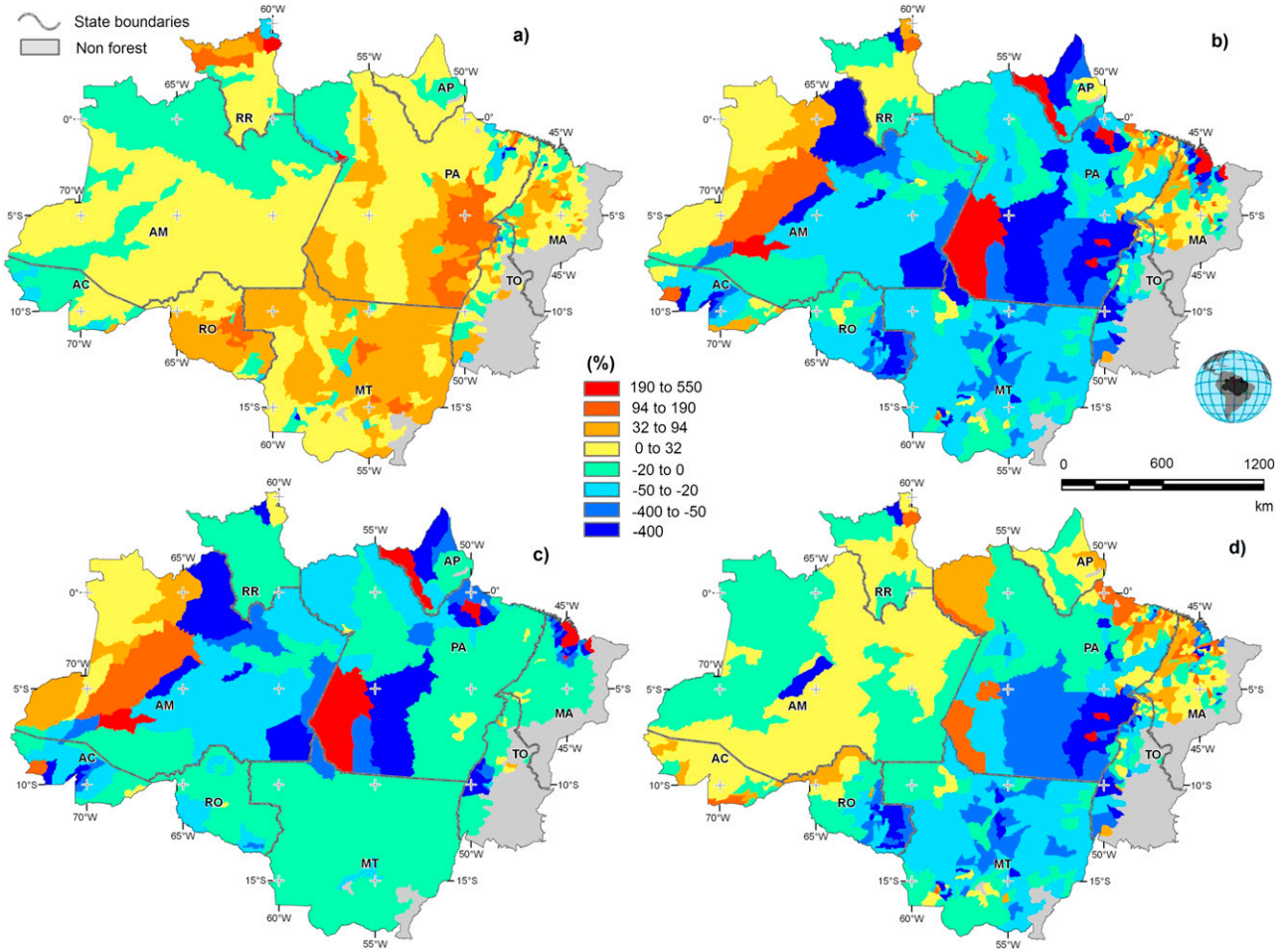

Fig. S4. Predicted variation in deforestation rates. (*A*) Predicted percent variation in deforestation rates from 2001–2004. (*B*) Predicted percent variation in deforestation rates from 2004 to 2006. (*C*) Difference (percent) in 2006 predicted deforestation rates, excluding the expansion of PAs within the period 2004–2006. (*D*) Difference (percent) in 2006 predicted deforestation rates, maintaining 2004 agricultural growth rates.

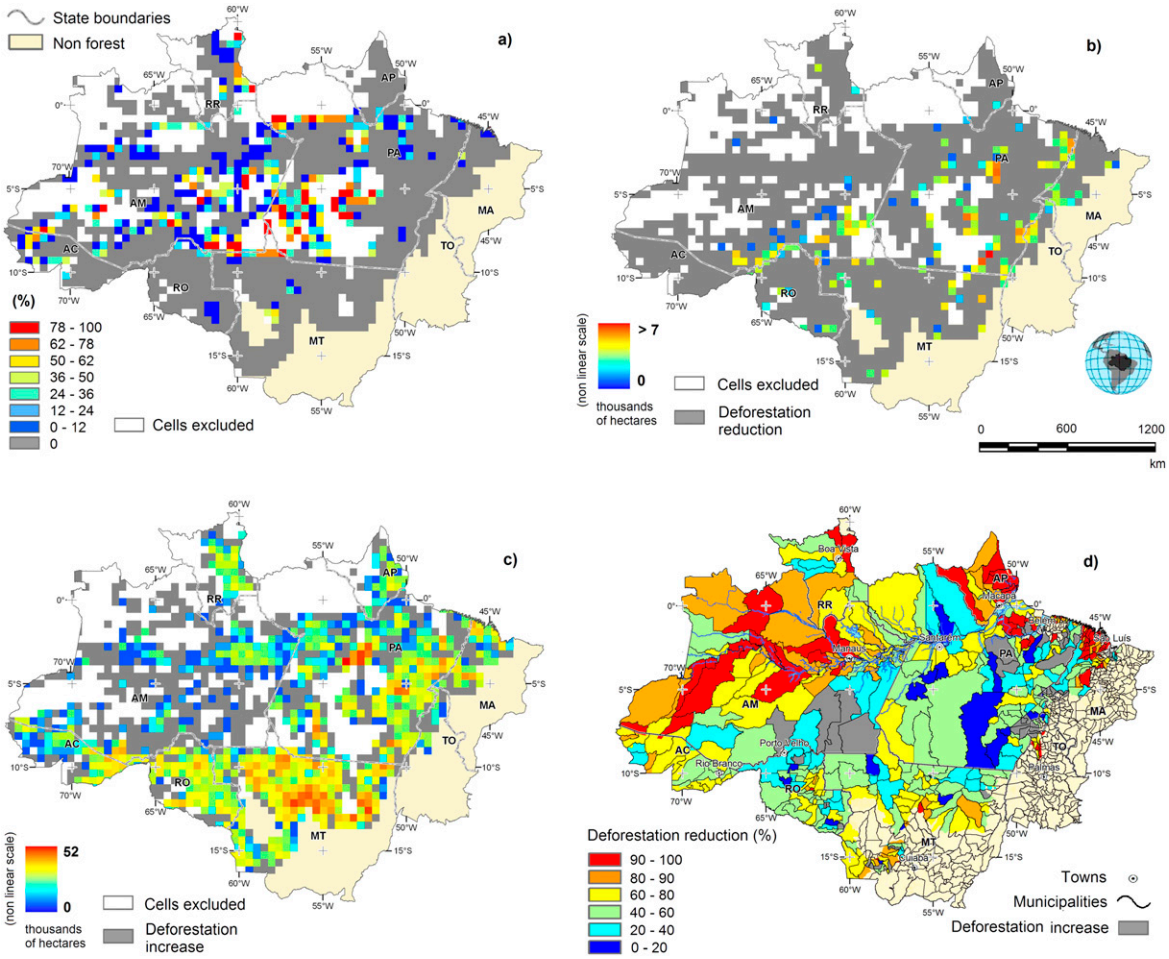

Fig. S5. PA expansion versus deforestation variation. (*A*) Percent of PA expansion from 2002–2007 within 50 × 50 km grid cells, excluding cells completely covered by PAs. (*B*) Increase in biennial deforestation rates outside PAs from 2002–2004 to 2005–2007. (*C*) Reduction in biennial deforestation rates outside PAs from 2002–2004 to 2005–2007. (*D*) Percent variation in biennial deforestation rates outside PAs from 2002–2004 to 2005–2007.

Other Supporting Information Files

Table S1 (DOCX)
Table S2 (DOCX)
Table S3 (DOCX)
Dataset S1 (XLSX)